Proceedings of the 8th European Conference of the Prognostics and Health Management Society 2024 - ISBN – 978-1-936263-40-0

Labeling Algorithm for Outer-Race Faults in Bearings Based on Load Signal

Tal Bublil[1, *], Cees Taal[2], Bert Maljaars[2], Renata Klein[3], Jacob Bortman[1]

[1] *PHM Laboratory, Department of Mechanical Engineering, Ben-Gurion University of the Negev, P.O.B653, Beer-Sheva 8410501, Israel*

talbub@post.bgu.ac.il
jacbort@post.bgu.ac.il

[2] *SKF, Research and Technology Development, Meidoornkade 14, 3992AE, Houten, the Netherlands.*

cees.taal@skf.com
bert.maljaars@skf.com

[3] *R.K. Diagnostics, P.O. Box 101, Gilon, D.N. Misgav 20103, Israel*

Renata.Klein@rkdiagnostics.co.il

ABSTRACT

Rolling element bearings are essential components for the proper functioning of many types of rotating equipment. Diagnosing faults in bearings has traditionally been done using signal processing techniques inspired by physics, wherein acceleration signals are analyzed using time-frequency analysis methods. To study the effect of bearing damage on acceleration signals, experiments are typically performed aiming for a natural propagation of a spall. However, the extent of spall severity during the test remains uncertain. It is possible to disassemble and reassemble the bearing for visual inspection. Nevertheless, previous studies observed that the vibration signal would drastically change if this operation was conducted repeatedly, impacting the identification of trends in the acceleration signal. The objective of this study is to provide a method which can assist with labeling the spall size in endurance tests without the necessity of disassembling and reassembling the test rig. To address this issue, a new algorithm, based on the load cell signal was developed to assess the spall size using low-speed measurements. This algorithm enables the identification of the circumferential angle at which the rolling element interacts with the spall and is only carrying a partial load. The algorithm has been validated through visual inspections conducted during the experiment. This algorithm makes it possible to estimate the spall size without the need for visual inspection in subsequent experiments. A labeled endurance test contributes to a better understanding of spall propagation, such as the effect of speed, load, and material properties on the propagation speed. This study demonstrates how the load signal can be used for fault labeling with relatively simple and common techniques. This approach will enable the tackling of advanced and more complex problems in future endeavors, such as fault severity estimation and even prognosis.

1. INTRODUCTION

Bearings play a crucial role in nearly all rotating machinery (Malla & Panigrahi, 2019), and monitoring their condition typically involves four stages: detection, identification, severity estimation, and prognosis (Bechhoefer & Schlanbusch, 2018). A substantial amount of research has been conducted on the subject, with a focus on the detection and identification stages, which have shown promising results. Bearing damage severity is typically defined as a function of overall vibration levels ((ISO), 2016). Unfortunately, these thresholds are very application dependent and difficult to generalize. A robust and objective method for severity estimation in bearings remains challenging.

One common approach to define severity is based on raceway spall size in the circumferential direction. Among the studies engaging spall size estimation, various types of sensor measurements are utilized. Common methods include accelerometers, some employing oil debris monitoring (ODM), and others utilizing optic fibers (Gazizulin et al., 2019; Madar et al., 2022; Medvedovsky et al., 2022). A review of different approaches is given in Zhang et al., 2022. Accelerometers are relatively common components in machinery due to their ease of installation. Methods based on accelerometers typically try to identify the entry and exit points of rolling elements from the spall within the time domain (Epps I K, 1991; Moazen-ahmadi & Howard, 2016; Sawalhi & Randall, 2011). Some of these studies employ low-pass filters to detect entry and exit events (Moazen Ahmadi et al., 2016), a practice that may pose challenges due to its reliance on a rule of thumb. Additionally, these methods are often detecting very small defects, whereas numerous applications involve significant spall sizes. There are also severity estimation methods which utilize condition indicators, which are then employed to calculate a health indicator (Gebraeel et al., 2004; Ma et al., 2012). These methods offer increased robustness in noisy conditions compared to the aforementioned methods since they consider trends based on multiple sensor recordings over time. However, establishing a direct link between health indicators and spall size in rotating machinery poses challenges, primarily due to missing ground truth values of its spall size during operation.

Studies that use ODM can estimate the spall size by calculating the total mass of debris particles originating from the bearing (Madar et al., 2022; Portal et al., 2022). However, to use this method, certain geometric assumptions are made which might be invalid. Optic fibers are used to measure the strain on the housing bearing, and by tracking the changes in the signal, it is possible to calculate the length of the spall (Medvedovsky et al., 2022). Nevertheless, both of these methods require expensive equipment and are not suitable for every test rig or machinery.

Emulating the topography of a spall is a challenging task. Consequently, studies that have explored severity estimation in bearings often rely on artificial spalls with less realistic rectangular shapes. However, the interaction between the rolling element (RE) in the bearing and the artificial spall could be significantly different from the interaction with a real spall, which may result in higher impulses in the acceleration signal than those observed in natural spalls (Zhang et al., 2021).

One approach to achieve naturally growing spalls is through endurance tests. Nevertheless, for measuring the spall size in acceleration algorithm validation, it is necessary to disassemble and reassemble the test rig, which can significantly alter the vibration signal (Smith & Randall, 2015). Recent studies have shown, that for specific test rig setups a load cell can act as a proximity measurement for displacement containing a distinctive pattern related to the spall geometry (Zhang et al., 2022). Moreover, an observation is made that the load-cell signal is less sensitive to the re-assembly of a bearing compared to acceleration.

In this study we propose a unique algorithm to estimate spall sizes in endurance tests using load signals, which can be obtained without visually inspecting the spall. The algorithm is implemented at low speeds, enabling validation of spall dimensions during endurance experiments.

2. EXPERIMENTAL SETUP

The endurance test was conducted in SKF Research and Technology Development (RTD). The test was performed on the R2 test rig (Harris, 2006), as shown in Figure 1, with the positions of the accelerometer and the load cell indicated. For measuring the rotational speed, a tachometer measuring two pulses per shaft rotation was used. In the experiment, two bearings were measured: the tested bearing, located on the left side of the test rig, and a reference intact bearing positioned on the right side of the test rig. Both bearings were monitored throughout the experiment. The algorithm developed in this study was primarily validated using the load-cell data acquired from the tested bearing on the left side. Throughout the experiment, sensor snapshots were recorded, defined as synchronized recordings of all sensors at a sample rate of 49152 Hz for 36 seconds.

To validate the load-based algorithm, a visual inspection was required. To simplify the process of disassembling and reassembling the test rig, a bearing with a design that allows easy access to the outer race was chosen. The selected bearing is a cylindrical roller bearing of the N209 ECP type. During the experiment, only a pure radial load is applied because this bearing type cannot sustain axial loads.

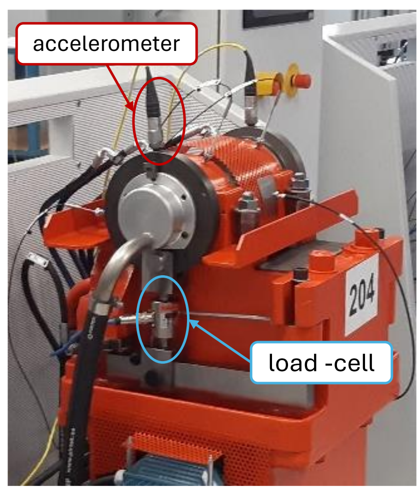

Figure 1: SKF R2 test rig; The accelerometer marked in red, load cell marked in blue.

2.1. Test Procedures

The test consists of two stages: (1) a damage initiation phase and (2) a spall growth phase. Both phases will be further explained in the following sections.

2.1.1. Damage Initiation Phase

In this phase, the purpose is to initiate a spall on the outer race of the bearing. To expedite this process, an initial small damage was introduced to the outer race before the test. The damage was created using an electrical discharge machine (EDM) on the race surface. The EDM created a rectangular-shaped damage with circumferential and axial dimensions of 0.2mm and 2mm, respectively. In this phase, the bearing was subjected to high loads and speeds to induce growth. The decision to stop this phase was made based on an acceleration-based condition indicator (Harris, 2006), where an abnormal increase determined the stopping criteria.

2.1.2. Spall Growth Phase

The objective of this phase is to capture snapshots of the data measured by the sensors while growing the spall at a controlled pace. The protocol of this phase contains three stages that repeat each other until the end of the experiment. Figure 2 illustrates one cycle of this protocol, which includes three stages: the growth stage in blue, the monitoring stage in orange, and the collection stage in green. The black and purple vertical lines at the bottom of the graph indicate the load in each stage (black for 16 kN and purple for 6 kN). The vertical axis represents the normalized duration, which is the time duration normalized by the combined time of the monitoring and collection stages. The vertical line represents the shaft speed.

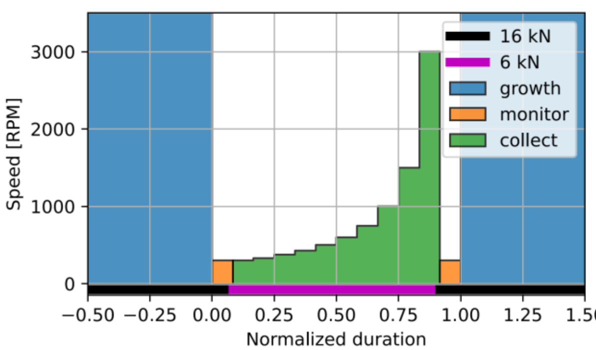

Figure 2: Example of one protocol cycle for spall growth. One cycle consists of three stages: 1: growth in blue, 2: monitor in orange, 3: collect in green.

In the growth stage, the aim is to accelerate spall growth; therefore, the bearing is subjected to a radial load of 16 kN, and the shaft rotational speed is set to 6000 RPM. One cycle of this stage lasts approximately 50 minutes.

In the monitor stage, two measurements are conducted at a high load with a speed of 300 RPM, one at the beginning of the collection stage and one at the end. In these measurements, the changes in the load cell are clearer and therefore will be used in this study for the load-based algorithm.

In the collection stage, measurements are taken from the sensors. In this phase, the load is reduced, and the speed changes to 10 different speeds spaced between 300 and 3000 RPM. The measurements at this stage will be used for future research. This stage takes around 20 minutes.

The experiment was halted approximately every 5 million revolutions for visual inspections. The test is stopped when a critical spall size, exceeding two times the distance between rolling elements, is reached. Beyond this size, two rolling elements no longer bear any load, which can lead to accelerated spall growth and, consequently, a high risk of critical failure.

3. Analysis of load cell signal

In a faulted bearing, with a spall not larger than the distance between two rolling elements in the outer race, the interaction of the rolling element and the spall can be roughly divided into two stages. In one stage, none of the rolling elements interacts with the spall. The other stage is when one of the rolling elements is interacting with the spall; both stages are illustrated in Figure **3**.

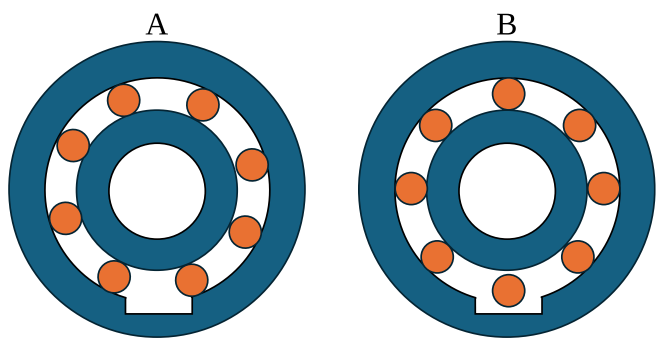

Figure 3: Illustration of REB interaction with outer race spall; (A) none of the RE interact with the spall (B) One RE enters the spall.

In stage one, the force applied to the bearing is divided among all the rolling elements in the bearing. In stage two, one of the rolling elements is inside the spall and, therefore, does not carry any load. This results in a different distribution of the load which appears to be observable on the load cell. By detecting these changes in the load cell, one can estimate the duration of the interaction with the spall, which can then be easily calculated to determine the spall length. At higher speeds, the transition between stages occurs more rapidly, meaning the system doesn't have enough time to stabilize, making it more challenging to detect in the time domain.

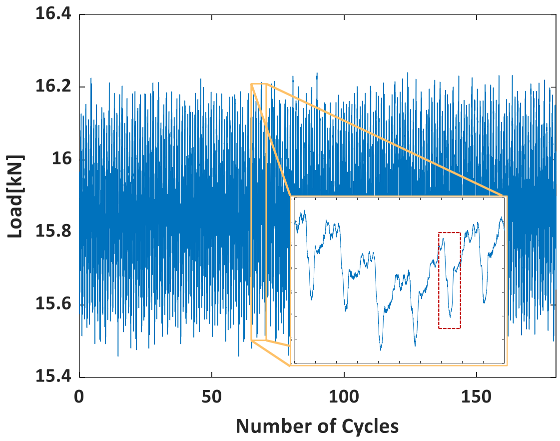

Figure 4: Raw load signal at 300 RPM with zoom on one cycle, equivalent to one shaft rotation: the area of interest marked by the red dashed rectangle indicate the area rolling element over the defect.

When examining the load signals acquired from the experiment at low speeds, it is possible to detect the interaction of the rolling element with the spall. Figure 4 shows an example of a signal with the visible interaction marked. To automate the process of identifying load distribution changes in the signal, a seven-step algorithm is proposed. The steps are described in Figure 6, with each step designed to emphasize and isolate the interaction of the rolling element with the spall. Each one of the steps is explained:

1. The load signal is detrended, by subtracting the "smoothed" signal from the original signal, making the signal centered around zero.

2. The interaction with the spall that occurs during the rotation of the shaft is periodic in the time domain when the speed is constant. However, even when setting the test rig to a constant speed, the speed is never truly constant. Therefore, angular resampling of the detrended load signal is conducted, converting the signal to the cycle domain.

3. Bearings are asynchronous components due to slippage (Sol et al., 2022). When employing Modified SA, as further explained in point 5, one can obtain a signal with isolated synchronous elements to the shaft's frequencies. By subtracting the SA signals from the original signal, the discrete shaft synchronous frequencies are removed, mitigating the interferences of other rotating components. This yields a signal containing only the asynchronous components. This algorithm is known as de-phase (Klein, 2017).

4. The cycle of interest is the interaction between the rolling element and the spall. Therefore, angular resampling is performed again based on the BPFO. Unlike the angular resampling based on the shaft's speed in step 2, the angular resampling in this step ensures a consistent number of samples in each cycle of the BPFO.

5. Modified Spectrum Analysis (MSA) (Koren, 2017) is utilized in this scenario. In MSA, the signal is segmented into N parts. The amplitudes of the Fourier Transforms (FT) for these segments are then averaged, resulting in an MSA signal with the averaged amplitude and phase information from a single segment. The fundamental steps of the MSA algorithm are outlined in Equations 1 and 2. Where N is the number of segments into which the signal is divided, and x_n represents a single segment of the signal. This technique is employed to isolate signal components asynchronous to the BPFO, including noise.

$$|\bar{X}| = \frac{1}{N}\sum_{n=1}^{N}|fft(x_n)| \quad (1)$$

$$MSA = ifft\{|\bar{X}| \cdot exp(j \cdot \angle fft(x_1))\} \quad (2)$$

6. A dynamic threshold is established by computing a percentage of the difference between the signal's highest and lowest points. Initially, a lower threshold is implemented for smaller spalls, which are more susceptible to noise interference. Once the estimated spall length reaches a predetermined value, a higher threshold is activated. This adjustment is intended to enhance accuracy. Figure 5 shows a processed signal with a set threshold indicated by a yellow dashed line.

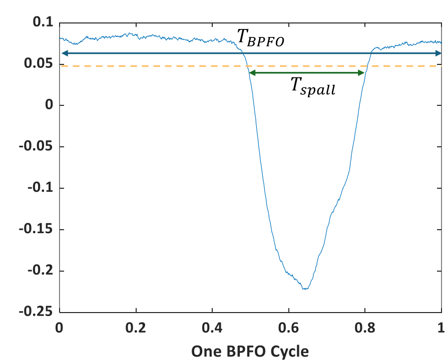

Figure 5: Processed signal with threshold indicated by a yellow dashed line; $\boldsymbol{T_{spall}}$ denotes the number of points below the threshold, and $\boldsymbol{T_{BPFO}}$ represents the total number of points in the MSA signal.

7. The determination of the pulse length involves calculating the percentage of values below the dynamic threshold. With the utilization of Equation 3, estimation of the spall size becomes feasible.

Here, RE represents the distance between two rolling elements, T_{spall} denotes the number of points in the synchronous average below the threshold, and T_{BPFO} represents the total number of points in the MSA signal.

$$S = RE \cdot \frac{T_{spall}}{T_{BPFO}} \tag{3}$$

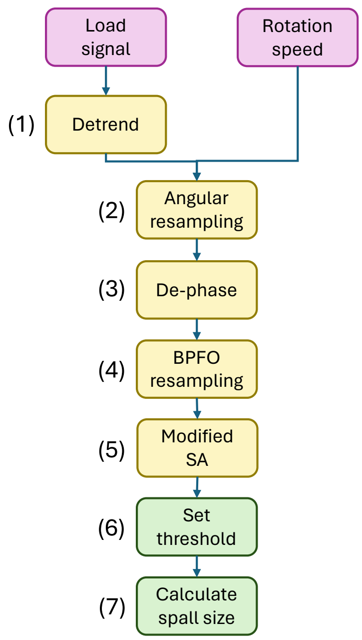

Figure 6: Block diagram of the load-based algorithm.

4. Results

To validate the load algorithm, visual inspections were conducted during the endurance experiment. The tested bearing is a SKF N209 ECP cylindrical roller bearing. During each visual inspection, only the outer ring was disassembled, examined, and photographed. The spall size was measured by counting the number of pixels the spall occupies in each photo. An example from two visual inspections is shown in Figure 7. The spall lengths calculated from the proposed algorithm and the visual inspections were plotted for comparison and presented in Figure 8.

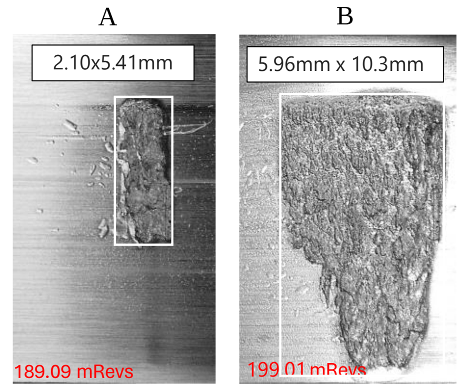

Figure 7: Visual inspections during endurance test: (A) at 189.09 million revolutions and (B) at 199.01 million revolutions. direction of the RE is from right to left.

It is evident that the estimated spall size by the load algorithm follows the trend of the measured sizes. However, in some cases, the estimated spall size deviates from that trend. These deviations sometimes occur after the visual inspections. The process of disassembling and reassembling could significantly alter the measured signals, as noted in a previous study (Heng et al., 2009). However, in the load signals, the impact is relatively small compared to acceleration and can be mitigated by using smoothing techniques. In other cases, the changes could be related to machinery malfunction, which contaminated the measurements. Despite these deviations, the suggested algorithm has shown good results and, in most cases, has been able to estimate the spall length accurately.

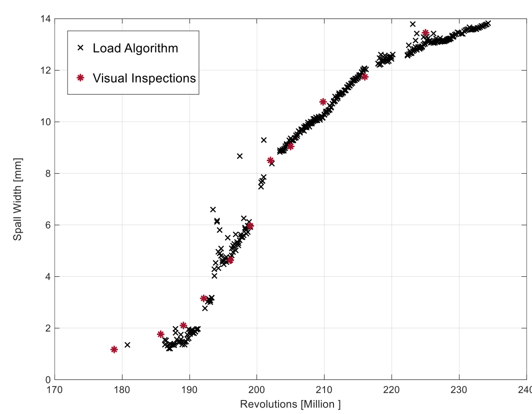

Figure 8: Comparison between the results of the load-based algorithm and the visual inspection.

In this work we present an algorithm to track spall size continuously in a robust manner in a lab environment by using existing load cells. Our proposed method can be used to validate spall size estimation algorithms. Moreover, it can be used to further study the physics of spall propagation, e.g., understanding the effects of speed and load.

5. CONCLUSION

In conclusion, bearings play a vital role in nearly all rotating machinery, highlighting the necessity of accurately estimating the severity of defects within them. As of today, there is no robust method for severity estimation in bearings, which can be used in all machinery. Endurance tests are crucial in bearing research, providing valuable insights into spall growth, and accurately labeling the data is essential for understanding this process.

Traditionally, labeling has relied on visual inspections during endurance tests, which can significantly alter vibration analysis results. This study introduces a load-based algorithm that eliminates the need for visual inspection, thus providing a more extensive dataset for labeling the severity of spalls. Although load cells are not typical components in machinery, they are common in experimental test rigs and can greatly assist with future research. The load-based algorithm was validated via visual inspection, demonstrating good agreement between the two methods. Not only does this algorithm streamline the testing process, but it also serves as a valuable tool for future studies, enabling researchers to track spall propagation and establish ground truth for developing acceleration-based algorithms. Overall, the implementation of this load-based algorithm represents a significant advancement in bearing defect analysis, offering improved labeling accuracy and opening up new avenues for further research in the field.

ACKNOWLEDGEMENT

Tal Bublil is supported by a scholarship sponsored by the Ministry of Science & Technology, Israel.

NOMENCLATURE

x_n	single segment of the signal
$\lvert\bar{X}\rvert$	average of the segment amplitudes
N	numbers of segments
MSA	MSA signal
RE	distance between two rolling elements
T_{spall}	number of points representing the spall
T_{BPFO}	total number of points in the MSA signal
S	spall length

REFERENCES

(ISO), I. S. O. (2016). *20816-1 Mechanical vibration - Measurement and evaluation of machine vibration - Part 1: General guidelines*.

Bechhoefer, E., & Schlanbusch, R. (2018). Calculating Remaining Useful Life in an Embedded System. *Proceedings of the Annual Conference of the Prognostics and Health Management Society, PHM*, 1–9.

Epps I K. (1991). *An investigation into vibrations excited by discrete faults in rolling element bearings.*

Gazizulin, D., Cohen, E., Bortman, J., & Klein, R. (2019). Critical Rotating Machinery Protection by Integration of a "fuse" Bearing. *International Journal of Critical Infrastructure Protection*, *27*, 100305.

Gebraeel, N., Lawley, M., Liu, R., & Parmeshwaran, V. (2004). Residual Life Predictions From Vibration-Based Degradation Signals: A neural network approach. *IEEE Transactions on Industrial Electronics*, *51*(3), 694–700.

Heng, A., Zhang, S., Tan, A. C. C., & Mathew, J. (2009). Rotating Machinery Prognostics: State of the art, challenges and opportunities. *Mechanical Systems and Signal Processing*, *23*(3), 724–739.

Klein, R. (2017). Comparison of Methods for Separating Vibration Sources in Rotating Machinery. *Mechanical Systems and Signal Processing*, *97*, 20–32.

N. Koren, I. Dadon,J. Bortman, R. Klein, (2017). Steps Towards Fault Prognostics of Gears. International Journal of Condition Monitoring, vol. 7, no. 1, pp.10-15.

Ma, L., Kang, J. S., & Zhao, C. Y. (2012). Research on Condition Monitoring of Bearing Health Using Vibration Data. *Applied Mechanics and Materials*, *226–228*, 340–344.

Madar, E., Galiki, O., Klein, R., Bortman, J., Nickell, J., & Kirsch, M. (2022). A New Model for Bearing Spall Size Estimation Based on Oil Debris. *Engineering Failure Analysis*, *134*(September 2021), 106011.

Malla, C., & Panigrahi, I. (2019). Review of Condition Monitoring of Rolling Element Bearing Using Vibration Analysis and Other Techniques. *Journal of Vibration Engineering and Technologies*, *7*(4), 407–414.

Medvedovsky, D., Ohana, R., Klein, R., Tur, M., & Bortman, J. (2022). Spall Length Estimation Based on Strain Model and Experimental FBG Data. *Mechanical Systems and Signal Processing*, *171*(February), 108923.

Moazen-ahmadi, A., & Howard, C. Q. (2016). A Defect Size Estimation Method Based on Operational Speed and Path of Rolling Elements in Defective Bearings. *Journal of Sound and Vibration*, *385*, 138–148.

Moazen Ahmadi, A., Howard, C. Q., & Petersen, D. (2016). The Path of Rolling Elements in Defective Bearings: Observations, Analysis and Methods to Estimate Spall Size. *Journal of Sound and Vibration*, *366*, 277–292.

Portal, O., Madar, E., Klein, R., Bortman, J., Nickell, J., & Kirsch, M. (2022). Towards Bearings Prognostics Based on Oil Debris. *Proceedings of the Annual*

Conference of the Prognostics and Health Management Society, PHM, *14*(1), 1–6.

Harris, T.A., & Kotzalas, M.N. (2006). Bearing Endurance Testing and Element Testing. (5th ed.) *Advanced Concepts of Bearing Technology: Rolling Bearing Analysis, Fifth Edition.* (763-792). Boca Raton.

Sawalhi, N., & Randall, R. B. (2011). Vibration Response of Spalled Rolling Element Bearings: Observations, Simulations and Signal Processing Techniques to Track the Spall Size. *Mechanical Systems and Signal Processing*, *25*(3), 846–870.

Smith, W. A., & Randall, R. B. (2015). Rolling Element Bearing Diagnostics Using the Case Western Reserve University data: A benchmark study. *Mechanical Systems and Signal Processing*, *64–65*, 100–131.

Sol, A., Madar, E., Bortman, J., & Klein, R. (2022). Autonomous Bearing Tone Tracking Algorithm. *PHM Society European Conference*, *7*(1), 466–472.

Zhang, H., Borghesani, P., Randall, R. B., & Peng, Z. (2022). A Benchmark of Measurement Approaches to Track the Natural Evolution of Spall Severity in Rolling Element Bearings. *Mechanical Systems and Signal Processing*, *166*(March 2021), 108466.

Zhang, H., Borghesani, P., Smith, W. A., Randall, R. B., Shahriar, M. R., & Peng, Z. (2021). Tracking the Natural Evolution of Bearing Spall Size Using Cyclic Natural Frequency Perturbations in Vibration Signals. *Mechanical Systems and Signal Processing*, *151*, 107376.

BIOGRAPHIES

Tal Bublil is currently a Ph.D. student in the BGU-PHM LAB at the Department of Mechanical Engineering in Ben-Gurion University of the Negev, under the supervision of Prof. Jacob Bortman. He completed his bachelor's degree with the highest honors in mechanical engineering at Ben-Gurion University of the Negev and completed his master's degree through the fast-track program.

Cees Taal has a research background with over ten years of experience in the field of sensor signal processing and machine learning. He has worked in academia (Delft University of Technology, Delft, The Netherlands, and KTH Royal Institute of Technology, Stockholm, Sweden) on audio and speech processing, after which he held various industrial positions in biomedical engineering (Philips Research, Eindhoven, Netherlands) and the energy domain (Eneco, Rotterdam, Netherlands). He is currently appointed as a Technologist of SKF, The Netherlands, where he is responsible for defining a research strategy in the field of bearing diagnostics and prognostics. Cees received the IEEE Signal Processing Society Best Paper Award in 2016.

Bert Maljaars is a researcher in SKF Research and Technology Development, working on diagnostics and prognostics in bearing condition monitoring. He received his MSc degree in Mechanical Engineering from Eindhoven University of Technology and afterwards his PhD degree (2017). His main research interests are state estimation, signal processing, physical modeling, optimization and control.

Renata Klein received her Ph.D. in the field of Signal Processing from the Technion, Israel Institute of Technology. For 17 years she managed the Vibration Analysis department in ADA-Rafael, the Israeli Armament Development Authority. Later, as the Chief Scientist in RSL- Electronics, she invented and led the development of a vibration based diagnostics and prognostics system that is used successfully in combat helicopters and UAVs of the Israeli Air Force. Renata is the CEO and owner of R.K. Diagnostics. In this role, and per invitation from Safran Aircraft Engines, she developed a full set of vibration based diagnostics and prognostics algorithms for jet engines. These algorithms are being integrated into the next generation of CFM jet engines. In recent years, Renata has focused on supervising academic research programs in the area of rotating machinery prognostics. Jointly with Prof. Jacob Bortman, she co-manages the BGU PHM Lab in Ben Gurion University of the Negev, teaches and provides supervision to MSc and PhD students.

Jacob Bortman is currently a full Professor in the department of mechanical engineering and the head of the PHM Lab in Ben-Gurion University of the Negev. Retired from the Israeli air force as brigadier general after 30 years of service with the last position of the head of material directorate. Chairman and member of several boards: director of business development of Odysight Ltd, Chairman of the board of directors, Selfly Ltd., board member of Augmentum Ltd., board member of Harel finance holdings Ltd., Chairman of the board of directors, Ilumigyn Ltd. Editorial board member of: "Journal of Mechanical Science and Technology Advances (Springer, Quarterly issue)". Head of the Israeli organization for PHM, IACMM - Israel Association for Comp. Methods in Mechanics, ISIG - Israel Structural Integrity Group, ESIS - European Structural Integrity Society. Received the Israel National Defense prize for leading with IAI strategic development program, Outstanding lecturer in BGU, The Israeli prime minister national prize for excellency and quality in the public service - First place in Israel. Over 80 refereed articles in scientific journals and in international conference.